JACS
JOURNAL OF THE AMERICAN CHEMICAL SOCIETY
pubs.acs.org/JACS
Article

Contrasteric Glycosylations of Cotylenol and 1,2-Diols by Virtual Linker Selection

Dylan W. Snelson,[#] Stephen I. Ting,[#] and Ryan A. Shenvi*

Cite This: J. Am. Chem. Soc. 2025, 147, 1327−1333
Read Online
ACCESS | Metrics & More | Article Recommendations | Supporting Information

ABSTRACT: Many terpene glycosides exhibit contrasteric patterns of 1,2-diol glycosylation in which the more hindered alcohol bears a sugar; protection of the less hindered alcohol only increases steric repulsion. Here, we report a method for contrasteric glycosylation using a new sugar-linker that forms a cleavable, 10-membered ring with high efficiency, leading to syntheses of cotylenin E, J, and ISIR-050. Linker selection was aided by DFT calculations of side reactions and stereoselectivity, as well as conformational analyses using autoDFT, a Python script that converts SMILES strings to DFT-optimized conformational ensembles.

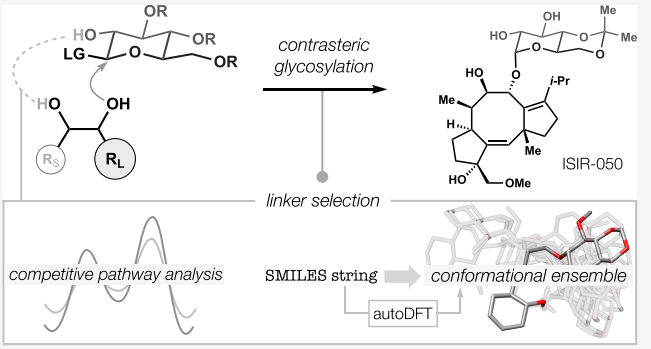

INTRODUCTION

The fusiccocane diterpenoids exert effects on eukaryotic cells—differentiation, neurite outgrowth and viability—by stabilization of PPIs between 14−3−3 proteins and client phosphoproteins, including disease relevant targets like C-RAF, p53, and BAD.[1−3] The cotylenins (Figure 1a) are of particular interest since cotylenin A (CNA, **1**) and its congeners induce differentiation of acute myeloid leukemia (AML) cells.[4,5] There have been four syntheses of the aglycon, cotylenol (**4**, Figure 1c), but cellular activity in differentiation and viability assays has required the full terpene glycoside (**1**−**3**).[6−14]

Biosynthetic glycosylation of the cotylenins occurs consistently at the hindered C9 secondary alcohol, whereas the more accessible C8 hydroxyl[15] remains unmodified across the classes.[16] This pattern of contrasteric 1,2-glycosylation can be found among diverse terpene glycosides (Figure 1a), but no general method for its synthesis has emerged.[17−19] An obvious solution would be to protect the more accessible hydroxyl and then glycosylate the remaining site. This strategy, however, increases the steric bulk around the already-hindered alcohol, only exacerbating the problem. Seminal work by Nakada, for example, provided the first and only chemical synthesis of a glycosylated cotylenol (cotylenin A, **1**) using this protecting group strategy.[7] Unfortunately, the 5-step protection/glycosylation/deprotection sequence yielded only 3% of **1** from the aglycone and impeded access to diverse congeners[7] (for other protecting group failures, see below and ref 20). In addition to the steric challenge, **1**−**4** decompose in the presence of Brønsted and Lewis acids, limiting compatibility with many glycosylation protocols.[21,22]

Rather than struggle against the unhindered C8 alcohol, we thought that it might be used strategically in a linker-based glycosylation. The use of a linker (i.e., molecular clamp,[23] tether,[24] or template[25] to guide glycosylation) has been successfully applied to oligosaccharide synthesis with site- and stereoselectivity.[26−28] In contrast to saccharides, however, terpene glycosides can exhibit far greater steric congestion, like tertiary alcohol attachment points or ring concavity, and pose specific challenges to chemo- and stereoselectivity. As a result, existing linkers were ineffective to glycosylate **4**. Below we detail our use of computational modeling to select an appropriate and general glycosylation linker (Figure 1c), leading to syntheses of cotylenin E, J, and ISIR-050, as well as a general method to access contrasteric terpene glycosides.

RESULTS AND DISCUSSION

Our initial efforts to glycosylate cotylenol (**1**) *inter*-molecularly proved unsuccessful. Attempts to faithfully reproduce Nakada's results using the Wan protocol with simple sugar donors did not generate any glycosylated products.[7,29] Variation of the leaving group, activation method, and protecting group pattern returned only the aglycone or caused extensive decomposition due to the acid instability of the core, even at high sugar concentrations. As a result, we considered methods for

Received: November 7, 2024
Revised: December 3, 2024
Accepted: December 4, 2024
Published: December 17, 2024

https://doi.org/10.1021/jacs.4c15719
J. Am. Chem. Soc. 2025, 147, 1327−1333

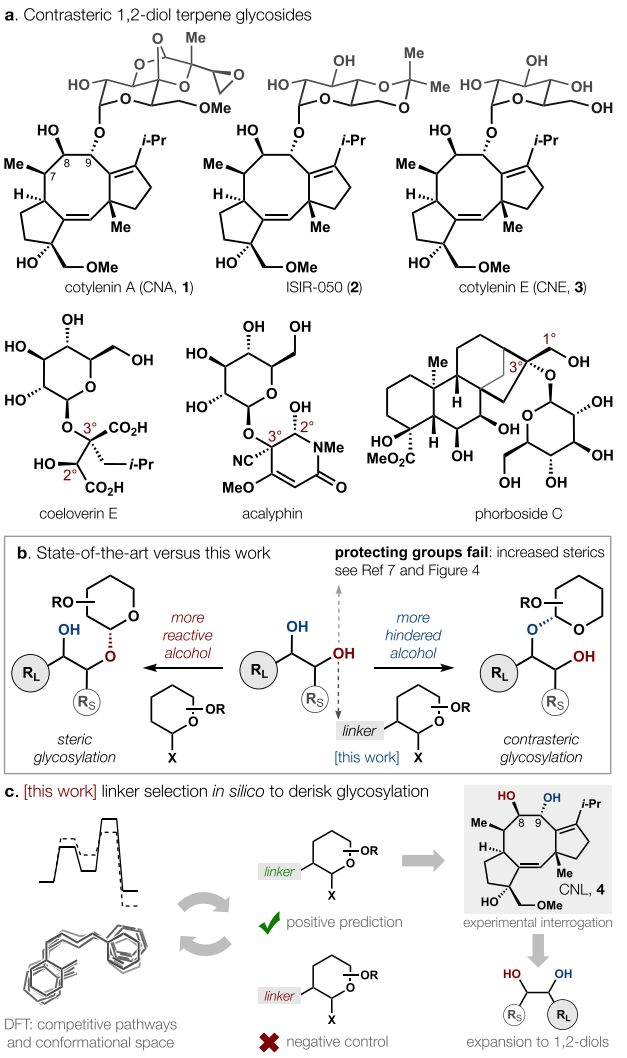

Figure 1. Cotylenin synthesis requires contrasteric glycosylation of 1,2-diol, a common motif among terpene glycosides.

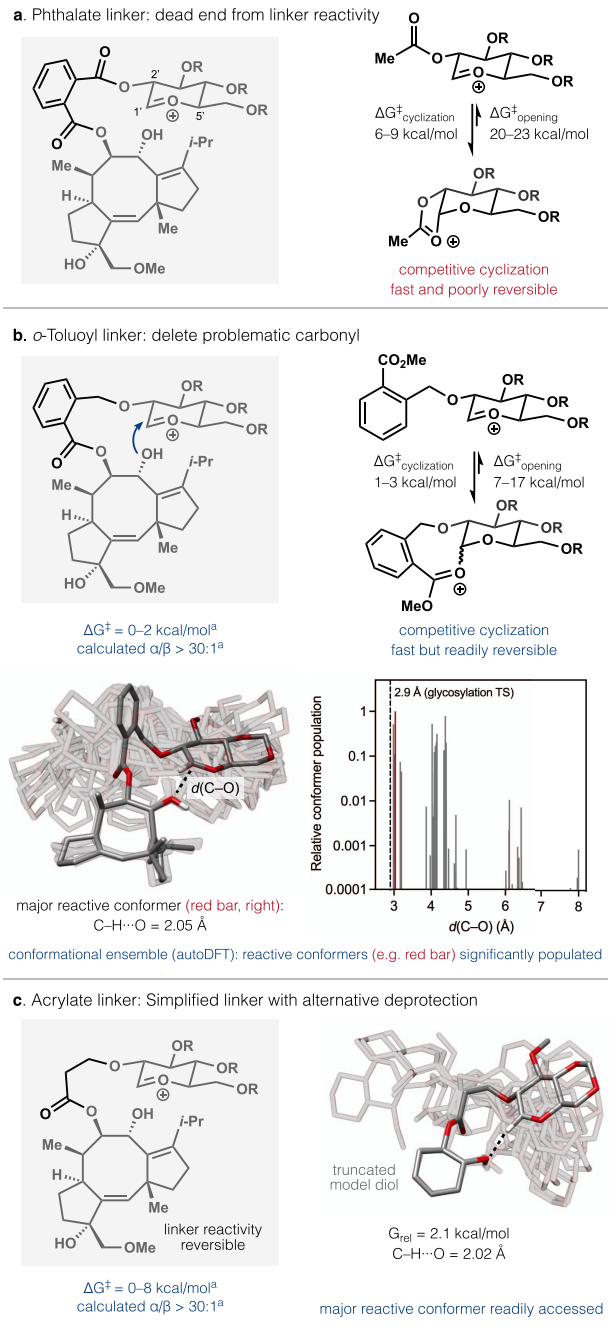

Figure 2. Triage of virtual linkers via analysis of on- vs off-pathway barriers, stereoselectivity, conformational space, and interatomic distance. See Supporting Information for full details.

oligosaccharide synthesis pioneered by Kusumoto,[30] Ziegler,[22,24] Demchenko[31,32] and others in which a "molecular clamp" enforced the proximity of two or more sugars to facilitate bond formation. In the context of cotylenol, we imagined a cleavable linker that would first engage the more reactive C8 hydroxyl and then deliver a sugar to its neighbor at C9. Unfortunately, tethered glycosylations have been reported only for oligosaccharide synthesis and not generalized to diverse acceptor motifs, especially hindered alcohols (Figure 1b). This is important because the structures of competent linkers—length, substitution pattern, ring content, etc.—are directly dictated by tether sites and stereochemical configurations of the two reacting sugars. These considerations complicated linker design/selection, especially given the unique structure and reactivity constraints of **4**. First, the linker would require placement at C2′[33,34] to accommodate sugar modifications at C3′-5′ that affect cellular activity.[12] Second, glycosylation would require α-selectivity (axial attack). Whereas simple succinate linkers at C2′ have led to α-linked disaccharides,[24] calculations suggested these would fail for hindered alcohols (see Figure 2), as we subsequently verified (see Figure 4).[35] Third, linker excision would require tolerance of the sensitive functional groups of **4**, placing further constraints on linker selection. Standard design cycles of trial and error were also complicated by small-scale experimentation, linker stability, protecting group compatibility, and analysis of macrocyclic (≥10-membered ring) product mixtures.

To maximize the chance of a successful tethered glycosylation, we evaluated possible linkers through a workflow with increasing fidelity to reality: physical and *in silico* models followed by DFT calculations of side reactivity, relative energies of stereoisomeric transition states, and ground state conformational ensembles (see Figure 2). This process was first applied to diester linkers, which benefited from commercial availability and straightforward methods of installation and cleavage. For example, Ziegler's succinyl and

https://doi.org/10.1021/jacs.4c15719
J. Am. Chem. Soc. 2025, 147, 1327−1333

phthaloyl linkers (both 4-atom spacers) seemed conducive to α-glycosylation in a physical model and a calculated ensemble of ground states (see Supporting Information Figure S7). However, transition state calculations indicated that an ester adjacent to the anomeric carbon would be ill-advised (Figure 2a): competitive cyclization to a dioxolenium cation would be poorly reversible at low temperature ($\Delta G^{\ddagger}_{opening}$ = 20−23 kcal/mol) and prevent α-selective macrocyclization.

An ester on the opposite terminus of the linker appeared less problematic, as its cyclization was predicted to be readily reversible even at low temperatures ($\Delta G^{\ddagger}_{opening}$ = 7−17 kcal/mol). We therefore considered the use of Schmidt's *o*-toluoyl linker, which was calculated to produce >30:1 α/β-selectivity ($\Delta\Delta G^{\ddagger}$ > 2.1 kcal/mol, see Supporting Information Figure S10) when modeled on *trans*-cyclohex-4-en-1,2-diol, whose diequatorial hydroxyls mimicked the dihedral angle of cotylenol (**4**). Importantly, the barrier to productive α-glycosylation of **4** was computed to be low (0−1 kcal/mol) and α-selective (30:1, α:β) (Figure 2b). Linker removal might then be affected by single-electron reduction and saponification.

We then evaluated the ground state conformational space of the acceptor-linker-sugar adduct as a proxy for the feasibility of macrocyclization (Figure 2c). To automate ground state DFT calculations with extensive conformer searching, we developed a Python-based program, autoDFT, designed for use by experimentalists with little to no experience with job submission on a high-performance computing cluster. AutoDFT requires the users to input molecules as SMILES strings, then automates conformer generation by CREST,[36] DFT calculations on the resulting conformers, and extraction and correction of thermodynamic data using Goodvibes.[37] Importantly, CREST achieves the effective sampling of ring conformers.

AutoDFT helped us understand the conformational landscape of a system that contained a sugar-derived oxocarbenium and the cotylenol core separated by a rotatable *o*-toluoyl linker. Together with several manually generated conformers, we located 63 conformers spanning 7 kcal/mol, of which 9 significantly populated structures corresponded to reactive conformations with C1'···C9−O distances (≤3.2 Å) nearing that of the glycosylation transition state (2.85 Å) (Figure 2c). The most populated reactive conformation exhibited typical conformational preferences (s-*trans* ester, minimized $A^{1,3}$-strain), and the oxocarbenium was stabilized by cation-π interactions and "nonclassical" CH···O hydrogen bond with the reacting alcohol (see Figure 2c). Together, these considerations suggested that the *o*-toluoyl linker preorganized the system for α-selective glycosylation.

We first appended the *o*-toluoyl sugar-linker conjugate to 2-methylpropane-1,2-diol to test its capacity for 11-membered ring formation (Scheme 1). Although the linker itself was used by Lemanski and Ziegler for the synthesis of oligosaccharides,[38,39] glycosylation of tertiary alcohols had not been probed. As suggested by the computational analysis above, macrocyclization occurred smoothly in 77% yield and >20:1 α:β selectivity. However, global deprotection by treatment with lithium naphthalenide according to Shia's procedure[40] yielded only small quantities of untethered product. Unfortunately, the same deprotection protocol was also ineffective using the cotylenol core, leading to extensive decomposition.

As an alternative, we investigated a 3-atom acrylate linker (Figure 2c) that might undergo cleavage via E1cb/solvolysis—

Scheme 1. Experimental Interrogation of the *o*-Toluoyl Linker

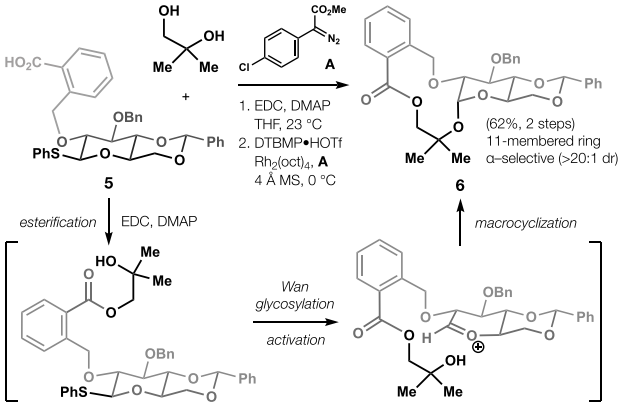

a strong base-mediated reaction[41] that seemed compatible with the reactivity constraints of **4**. Acrylates, however, were unprecedented for tethered glycosylation and lacked the geometric (planar *ortho*-arene) constraints of the *o*-toluoyl linker. Like the *o*-toluoyl linker, the acrylate demonstrated readily reversible ester macrocyclization ($\Delta G^{\ddagger}_{opening}$ = 13.5−14 kcal/mol, Supporting Information Figure S11) and a significant population of conformers that possessed close C1'···C9-OH interatomic distances (≤3.2 Å) as well as an oxocarbenium CH···O hydrogen bond (see Figure 2c). For speed of calculation, we initially explored the *trans*-cyclohex-4-en-1,2-diol model system, but the cotylenol core exhibited similar tendencies to favor α-glycosylation with low transition state barriers ($\Delta G^{\ddagger}$ = 0−8 kcal/mol). This favorability between the two related systems suggested a generality to the unprecedented acrylate linker that could be probed experimentally (see below).

The synthesis of acrylate-sugar conjugates involved a facile Cs_2CO_3-mediated oxy-Michael addition of sugar derivative **7**[42] to *tert*-butyl acrylate, affording **8** in 80% yield (Scheme 2). *Para*-methoxyphenyl (PMP) acetal and *para*-methoxybenzyl (PMB) protecting groups maximized divergency (see below) to access different sugar-linker conjugates from a common intermediate. Consequently, **8** served as a common entry into CNE, CNJ, and ISIR-050, as well as diverse glucosylated terpene diols (see Figure 3).

For example, global deprotection of **8** by DDQ and peracetylation occurred in a 66% yield. Acetyl was chosen so that its removal would occur in concert with methoxide-mediated linker cleavage. Selective *tert*-butyl ester heterolysis was effected with TFA to free the acid for diol coupling, providing the CNJ conjugate (**10**) in 89% yield. It is important to note that the reversal of choreography (dealkylation/peracetylation) led to unproductive and irreversible ε-lactone formation. Conversion of **8** to its dimethyl acetal (2,2-DMP, PTSA) occurred after DDQ deprotection (88% yield over 2 steps). The remaining free hydroxy group was acetylated (85%) to provide **11**, which was dealkylated using the same conditions as those above to arrive at the ISIR-050 conjugate (**12**) in 61% yield. Alternatively, acid-mediated acetal cleavage followed by Sugai's selective *O*6-methylation with Meerwein's salt provided **13** in 69% yield over two steps.[43] Deprotection of the remaining PMB group with DDQ followed by peracetylation/dealkylation delivered the CNE sugar-linker conjugate **14** in 78% yield over the final three steps. The

https://doi.org/10.1021/jacs.4c15719
J. Am. Chem. Soc. 2025, 147, 1327−1333

Scheme 2. Syntheses Sugar-Linker Conjugates, Interrogation of Predictions and Application to Cotylenin E, Cotylenin J, and ISIR-050[a]

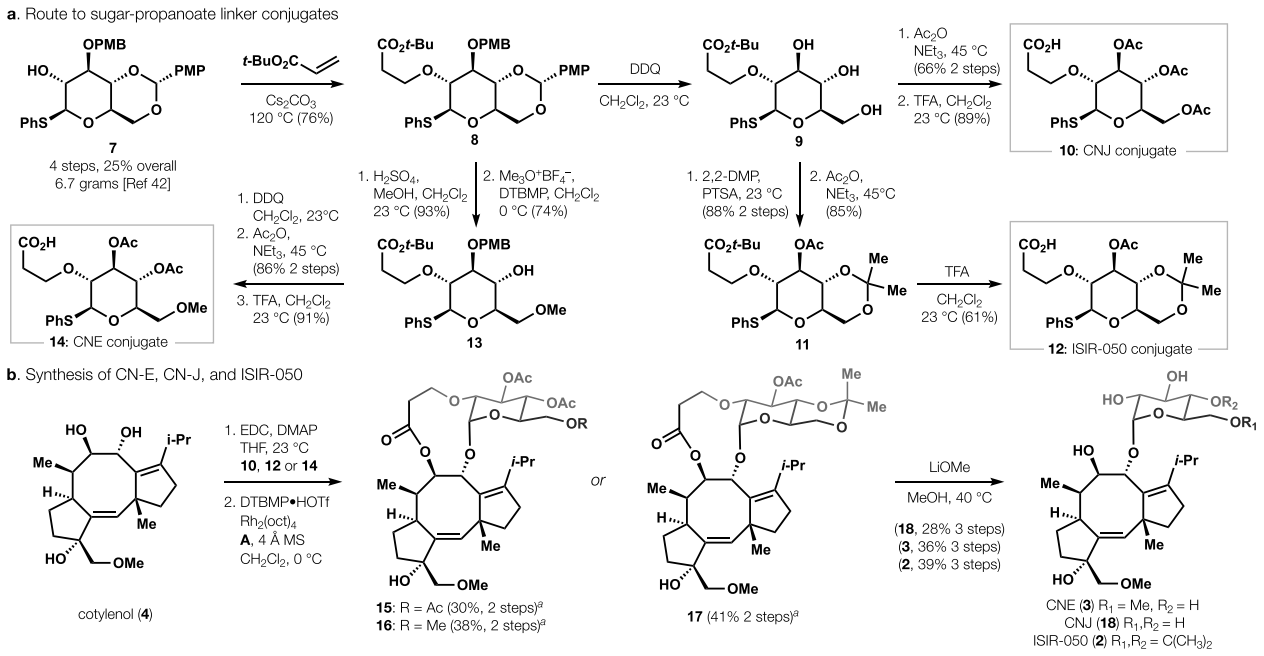

[a]>20:1 dr (α:β selectivity).

brevity and scalability of this route allowed extensive experimentation across both cotylenol and a collection of 1,2-diols.

Each sugar-linker conjugate (**10**, **12**, and **14**) reacted with cotylenol (**4**) using EDC and DMAP to provide **15**, **16**, and **17** with regioselectivity for the accessible C8 hydroxyl over C9. The esterification required careful control of stoichiometry (1:1 cotylenol: sugar-linker conjugate) to prevent sugar-linker dimerization (symmetric anhydride) and double esterification. Subjection to Wan's glycosylation protocol led to macrocyclization with only the α anomer observed (crude ^{1}H NMR), as suggested by DFT calculations of acrylate-cyclohexenediol models. The glycosylations were rapid (30 min) and successful on small scales (~1 μmol) at high dilution (1 mM), where adventitious water often can be problematic. The glycosylated macrocyles were globally deacetylated using LiOMe, which also served to remove the linker via methanolysis of the C8 ester and E1cB of the acrylate glucosyl ether, which provided the three cotylenin natural products with good efficiency from aglycone **4**. The 28−39% yield of this 3-step sequence using novel acrylate sugar-linker cassette **8** compares favorably to the existing 3%, 5-step protection/glycosylation/deprotection of cotylenol (**4**).[7]

Furthermore, the diversifiable sugar-linker cassette **19** could mediate the contrasteric glycosylation of diverse 1,2 diols via a 10-membered ring formation (Figure 3). Despite significant reductions in complexity between **4** and the simplest 1°/3° diol, isobutene glycol (351.25 vs 48.34 mcbits[44]), cyclization occurred with similar efficiency and selectivity (>20:1 α:β). Nevertheless, more complex 1°/3° diols also macrocyclized efficiently, even an acid-sensitive, dihydroxylated caryophyllene derivative,[45] which generated spiro-*bis*-macrocycle **23** diastereoselectively and in good yield (silica gel chromatography of the diol-linker-sugar intermediate was avoided due to acid sensitivity). More hindered 2°/3° diols cyclized equally well, as the driving forces for α/β-selectivity were unchanged, resulting in efficient contrasteric glycosylations of (−)-pinene-2,3-diol (**21**) and 3-carene-3,4-diol (**24**). Bifunctional or polyfunctional compounds led to spiroazetidine or tutin macrocycles **22** and **25**; the latter represents a potential lead to access tutin glycosides, which have never been prepared or modified to probe neuroactivity.

Yields of these macrocycles ranged from 44−73% over 2 steps and their formation could be conducted on a very small scale (0.01 mmol)—an asset for a multistep synthesis or diversification campaign. Even so, the reaction to form **21** could also be run on a 0.2 mmol scale (80% yield). Like the cotylenin macrocycles, cleavage of the linker at both attachment points could be achieved with lithium methoxide in this case to deliver differentially protected contrasteric terpene glycoside **26**. In contrast to cotylenins **2**, **3**, and **16**, none of the compounds **20**−**26** are *trans*-diequatorial-1,2-diols, suggesting that the acrylate linker may be applicable to diverse glycosylation problems in ways that other linkers are not (see Figure 4).

Control Experiments. The yield, regioselectivity, and stereoselectivity of the acrylate linker-controlled glycosylation contrasted starkly to intermolecular variations and the precedented succinate linker[22,24,25,38,46] for oligosaccharide synthesis (Figure 4). For example, intermolecular glycosylation of **27** generated, as expected, the opposite regioisomer (**28**) in which the sugar oxocarbenium ion reacted with the more accessible 1° alcohol. Furthermore, only the β-anomer was observed, even using C2′-ethereal protecting groups: a powerful demonstration of α-selectivity imparted by the acrylate linker. Very hindered systems like pinane-*cis*-2,3-diol (**29**) delivered no glycosylated product via intermolecular reaction (contrast to **21**, Figure 3). Similarly, protection of accessible alcohols such as **27** with a small acetyl group inhibited glycosylation: no desired product of either anomer

https://doi.org/10.1021/jacs.4c15719
J. Am. Chem. Soc. 2025, 147, 1327−1333

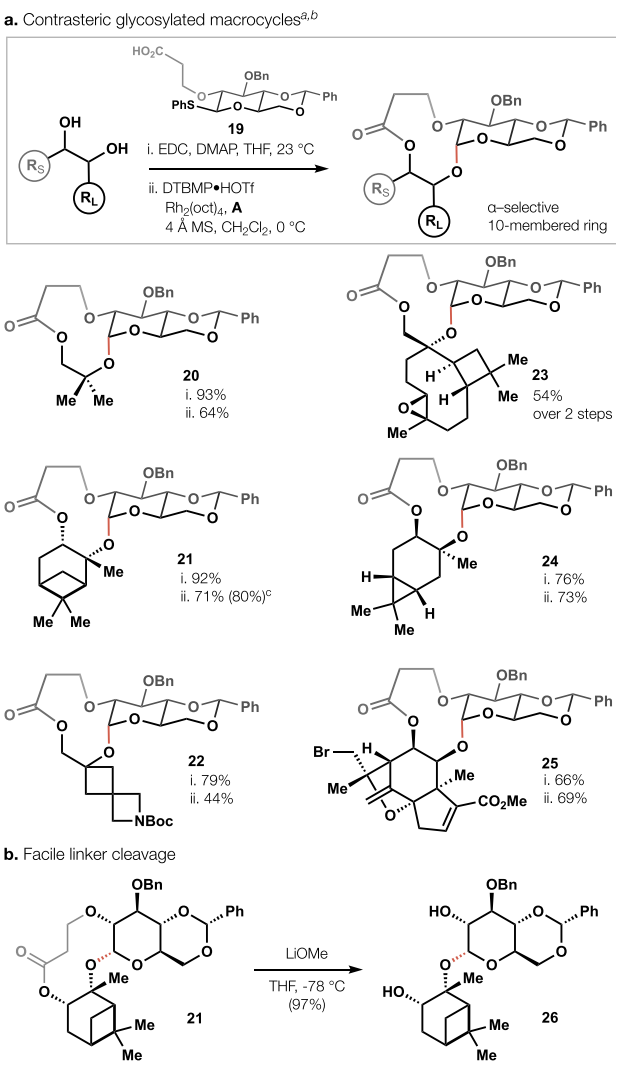

Figure 3. Scope across sterically differentiated 1,2-diols. [a]Isolated yield on 0.01 mmol scale; [b]α:β selectivity >20:1 in all cases; [c]Isolated yield on 0.2 mmol scale.

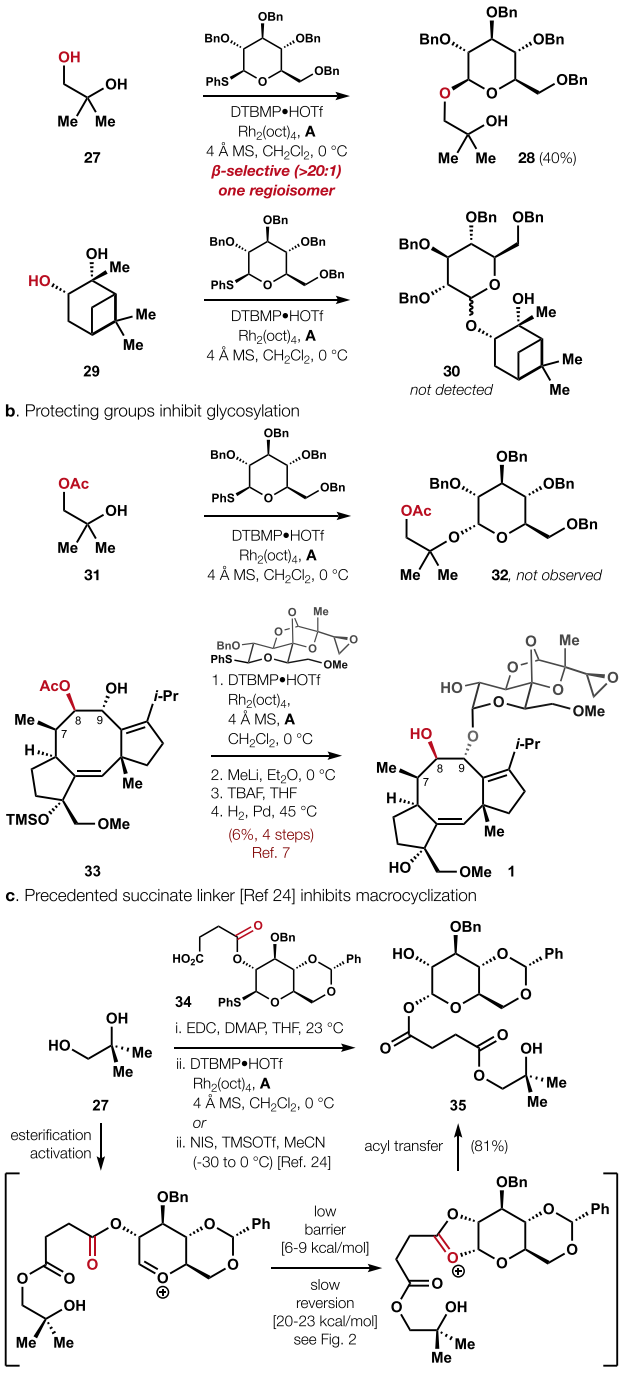

Figure 4. Control experiments: no linker, protecting groups, and precedented linkers are all ineffective. DTBMP: 2,6-di-*tert*-butyl-4-methylpyridine. For the structure of **A**, see Scheme 1.

was observed (contrast to Figure 3, entry **20**). This result mirrors the low yield associated with intermolecular glycosylation[29] of doubly protected cotylenol (**33**) (as noted in ref 7, large impurities in the protected intermediates make the glycosylation yield hard to determine). Finally, the use of the precedented succinate linker (Figure 4c), which computational analysis had discouraged due to the possibility of an irreversible five-membered ring formation, led to acyl transfer instead of macrocyclization. This is consistent with the favorable and poorly reversible oxocarbenium capture by the adjacent ester, as predicted (Figure 2).

■ CONCLUSIONS

We have developed a cleavable acrylate linker for the contrasteric glycosylation of 1,2 diols. This method enabled the robust glycosylation of the cotylenol C9 hydroxyl leading to cotylenin E (**3**), cotylenin J (**18**), and ISIR-050 (**2**). These complex glycosides are now being used as positive controls to benchmark SAR trends in 14−3−3 protein/client stabilization. Because the idiosyncratic donor and acceptor did not map well onto linkers developed for oligosaccharides, we derisked the linker selection by calculation of on- and off-pathway barriers as well as the analysis of conformational ensembles and their interatomic distances. That triage process quickly arrived at *o*-toluoyl and acryloyl linkers, which proved successful. In contrast, the well-precedented phthaloyl and succinyl linkers were predicted to fail. To check these predictions, we explored the succinate linker and indeed found that it led to unproductive acyl transfer. It is important to note that the acrylates can be carried through multiple steps of sugar modification, allowing divergence to a variety of possible sugars while serving as both a protecting group and a linker. Given the diversity of glycosylated terpenoids produced in

https://doi.org/10.1021/jacs.4c15719
J. Am. Chem. Soc. 2025, 147, 1327−1333

nature, we anticipate that other custom linkers will be necessary for future work.

The computational triage described here may benefit linker design-make-test cycles, especially the quick generation of conformer ensembles by the autoDFT script (available for download on GitHub,[47] along with instructions and customization options). Similar workflows[48] have been expedited in our group by autoDFT, which can be implemented by nonexperts to provide ground-state collections of analogs at high levels of theory.[49] This integration of computational tools with complex molecule synthesis at both strategic and tactical levels allows greater exploration over shorter times and promises to transform synthesis in the coming years.

■ ASSOCIATED CONTENT

Supporting Information

The Supporting Information is available free of charge at https://pubs.acs.org/doi/10.1021/jacs.4c15719.

Experimental procedures, characterization data, and structural assignments (PDF)
dft_xyz_files (ZIP)

■ AUTHOR INFORMATION

Corresponding Author

Ryan A. Shenvi − *Department of Chemistry, The Scripps Research Institute, La Jolla, California 92037, United States; Skaggs Graduate School of Chemical and Biological Sciences, La Jolla, California 92037, United States;* orcid.org/0000-0001-8353-6449; Email: rshenvi@scripps.edu

Authors

Dylan W. Snelson − *Department of Chemistry, The Scripps Research Institute, La Jolla, California 92037, United States; Skaggs Graduate School of Chemical and Biological Sciences, La Jolla, California 92037, United States*

Stephen I. Ting − *Department of Chemistry, The Scripps Research Institute, La Jolla, California 92037, United States*

Complete contact information is available at: https://pubs.acs.org/10.1021/jacs.4c15719

Author Contributions

#D.W.S. and S.I.T. contributed equally.

Notes

The authors declare no competing financial interest.

■ ACKNOWLEDGMENTS

We thank Umicore for their generous donation of Hoveyda-Grubbs 2nd generation catalyst [301224-40-8] used in the preparation of cotylenol (**4**). Dr. L. Pasternack and Dr. G. Koon are acknowledged for NMR assistance, as is Mr. Chunyu Li for providing the precursor 1,2-diol leading to **23**. We are grateful to Dr. M. Nasar, Dr. B. Smith, and Dr. N. Traux for helpful discussions about glycoside purification. The Scripps Automated Synthesis Facility performed HRMS analysis. Support was provided by the NSF (CHE 2155228 to R.A.S. and GRF 2235200 to D.W.S.) and the National Institutes of Health (R35 GM122606 to R.A.S. and F32 CA278405 to S.I.T.).

■ REFERENCES

(1) Hermeking, H. The 14−3-3 Cancer Connection. *Nat. Rev. Cancer* **2003**, *3* (12), 931−943.
(2) Molzan, M.; Kasper, S.; Röglin, L.; Skwarczynska, M.; Sassa, T.; Inoue, T.; Breitenbuecher, F.; Ohkanda, J.; Kato, N.; Schuler, M.; Ottmann, C. Stabilization of Physical RAF/14−3-3 Interaction by Cotylenin A as Treatment Strategy for RAS Mutant Cancers. *ACS Chem. Biol.* **2013**, *8* (9), 1869−1875.
(3) Doveston, R. G.; Kuusk, A.; Andrei, S. A.; Leysen, S.; Cao, Q.; Castaldi, M. P.; Hendricks, A.; Brunsveld, L.; Chen, H.; Boyd, H.; Ottmann, C. Small-Molecule Stabilization of the P53−14−3-3 Protein-Protein Interaction. *FEBS Lett.* **2017**, *591* (16), 2449−2457.
(4) Yamada, K.; Honma, Y.; Asahi, K.; Sassa, T.; Hino, K.; Tomoyasu, S. Differentiation of Human Acute Myeloid Leukaemia Cells in Primary Culture in Response to Cotylenin A, a Plant Growth Regulator. *Br. J. Hamaetol.* **2001**, *114* (4), 814−821.
(5) Asahi, K.; Honma, Y.; Hazeki, K.; Sassa, T.; Kubohara, Y.; Sakurai, A.; Takahashi, N. Cotylenin A, a Plant-Growth Regulator, Induces the Differentiation in Murine and Human Myeloid Leukemia Cells. *Biochem. Biophys. Res. Commun.* **1997**, *238* (3), 758−763.
(6) Kato, N.; Okamoto, H.; Takeshita, H. Total Synthesis of Optically Active Cotylenol, a Fungal Metabolite Having a Leaf Growth Activity. Intramolecular Ene Reaction for an Eight-Membered Ring Formation. *Tetrahedron* **1996**, *52* (11), 3921−3932.
(7) Uwamori, M.; Osada, R.; Sugiyama, R.; Nagatani, K.; Nakada, M. Enantioselective Total Synthesis of Cotylenin A. *J. Am. Chem. Soc.* **2020**, *142* (12), 5556−5561.
(8) Ting, S. I.; Snelson, D. W.; Huffman, T. R.; Kuroo, A.; Sato, R.; Shenvi, R. A. Synthesis of (−)-Cotylenol, a 14−3-3 Molecular Glue Component. *J. Am. Chem. Soc.* **2023**, *145* (37), 20634−20645.
(9) Jiang, Y.; Renata, H. Modular Chemoenzymatic Synthesis of Ten Fusicoccane Diterpenoids. *Nat. Chem.* **2024**, *16*, 1531−1538.
(10) Andlovic, B.; Heilmann, G.; Ninck, S.; Andrei, S. A.; Centorrino, F.; Higuchi, Y.; Kato, N.; Brunsveld, L.; Arkin, M.; Menninger, S.; Choidas, A.; Wolf, A.; Klebl, B.; Kaschani, F.; Kaiser, M.; Eickhoff, J.; Ottmann, C. IFNα Primes Cancer Cells for Fusicoccin-Induced Cell Death via 14−3-3 PPI Stabilization. *Cell Chem. Biol.* **2023**, *30* (6), 573−590.e6.
(11) Andrei, S. A.; de Vink, P.; Sijbesma, E.; Han, L.; Brunsveld, L.; Kato, N.; Ottmann, C.; Higuchi, Y. Rationally Designed Semisynthetic Natural Product Analogues for Stabilization of 14−3-3 Protein−Protein Interactions. *Angew. Chem., Int. Ed.* **2018**, *57* (41), 13470−13474.
(12) Inoue, T.; Higuchi, Y.; Yoneyama, T.; Lin, B.; Nunomura, K.; Honma, Y.; Kato, N. Semisynthesis and Biological Evaluation of a Cotylenin A Mimic Derived from Fusicoccin A. *Bioorg. Med. Chem. Lett.* **2018**, *28* (4), 646−650.
(13) Sassa, T.; Togashi, M.; Kitaguchi, T. The Structures of Cotylenins A, B, C, D and E. *Agric. Biol. Chem.* **1975**, *39* (9), 1735−1744.
(14) Sasa, T.; Sakata, Y.; Nukina, M.; Ikeda, M. Germination-inducing activity and chemical structure of cotylenin. *J. Chem. Soc. Jpn (Chem. Ind. Chem.)* **1981**, *1981* (5), 895−898.
(15) For example, acetylation and various esterifications occur selectively at C8.
(16) Guan, Z. Z.; Yao, N.; Yuan, W.; Li, F.; Xiao, Y.; Rehmutulla, M.; Xie, Y.; Chen, C.; Zhu, H.; Zhou, Y.; Tong, Q.; Xiang, Z.; Ye, Y.; Zhang, Y. Total Biosynthesis of Cotylenin Diterpene Glycosides as 14−3-3 Protein-Protein Interaction Stabilizers. *Chem. Sci.* **2024**,
(17) Huang, S.-Y.; Li, G.-Q.; Shi, J.-G.; Mo, S.-Y.; Wang, S.-J.; Yang, Y.-C. Chemical Constituents of the Rhizomes of Coeloglossum Viride Var Bracteatum. *J. Asian Nat. Prod. Res.* **2004**, *6* (1), 49−61.
(18) Kim, K. H.; Choi, S. U.; Lee, K. R. Diterpene Glycosides from the Seeds of Pharbitis Nil. *J. Nat. Prod.* **2009**, *72* (6), 1121−1127.
(19) Nahrstedt, A.; Kant, J.-D.; Wray, V. Acalyphin, a Cyanogenic Glucoside from *Acalypha Indica*. *Phytochemistry* **1982**, *21* (1), 101−105.
(20) Van Der Vorm, S.; Hansen, T.; Van Hengst, J. M.; Overkleeft, H. S.; Van Der Marel, G. A.; Codée, J. D. Acceptor reactivity in glycosylation reactions. *Chem. Soc. Rev.* **2019**, *48*, 4688−4706.
(21) Li, Y.; Yang, X.; Liu, Y.; Zhu, C.; Yang, Y.; Yu, B. Gold(I)-Catalyzed Glycosylation with Glycosyl Ortho-Alkynylbenzoates as

Donors: General Scope and Application in the Synthesis of a Cyclic Triterpene Saponin. *Chem.—Eur. J.* **2010**, *16* (6), 1871−1882.
(22) Lau, R.; Schüle, G.; Schwaneberg, U.; Ziegler, T. Prearranged Glycosides, 2. Intramolecular Glycosylation of Prearranged Saccharides as a Novel Strategy for the Construction of β-L-Rhamnosidic Linkages. *Liebigs Ann.* **1995**, *1995* (10), 1745−1754.
(23) Wakao, M.; Fukase, K.; Kusumoto, S. Chemical Synthesis of Cyclodextrins by Using Intramolecular Glycosylation. *J. Org. Chem.* **2002**, *67* (23), 8182−8190.
(24) Ziegler, T.; Lemanski, G.; Rakoczy, A. Anomeric Selectivity during Intramolecular Mannosylation of Succinyl Bridged Glycosides 1. *Tetrahedron Lett.* **1995**, *36* (49), 8973−8976.
(25) Valverde, S.; Gómez, A. M.; Hernández, A.; Herradón, B.; López, J. C. A Novel Strategy for Regio- and Stereo-Control in Glycosylation Reactions: Template-Directed Cyclo-Glycosylation of Monosaccharides. *J. Chem. Soc. Chem. Commun.* **1995**, *19*, 2005−2006.
(26) Jia, X. G.; Demchenko, A. V. Intramolecular Glycosylation. *Beilstein J. Org. Chem.* **2017**, *13* (1), 2028−2048.
(27) Ishiwata, A.; Joo Lee, Y.; Ito, Y. Recent Advances in Stereoselective Glycosylation through Intramolecular Aglycon Delivery. *Org. Biomol. Chem.* **2010**, *8* (16), 3596−3608.
(28) Cumpstey, I. Intramolecular Aglycon Delivery. *Carbohydr. Res.* **2008**, *343* (10), 1553−1573.
(29) Meng, L.; Wu, P.; Fang, J.; Xiao, Y.; Xiao, X.; Tu, G.; Ma, X.; Teng, S.; Zeng, J.; Wan, Q. Glycosylation Enabled by Successive Rhodium(II) and Brønsted Acid Catalysis. *J. Am. Chem. Soc.* **2019**, *141* (30), 11775−11780.
(30) Kusumoto, S.; Imoto, M.; Ogiku, T.; Shiba, T. Synthesis of β(1−4)-Linked Disaccharides of N-Acetylglucosamine and N-Acetylmuramic Acid by Their Direct Condensation. *Bull. Chem. Soc. Jpn.* **1986**, *59* (5), 1419−1423.
(31) Pornsuriyasak, P.; Jia, X. G.; Kaeothip, S.; Demchenko, A. V. Templated Oligosaccharide Synthesis: The Linker Effect on the Stereoselectivity of Glycosylation. *Org. Lett.* **2016**, *18* (9), 2316−2319.
(32) Jia, X. G.; Pornsuriyasak, P.; Demchenko, A. V. Templated Oligosaccharide Synthesis: Driving Forces and Mechanistic Aspects. *J. Org. Chem.* **2016**, *81* (24), 12232−12246.
(33) Partridge, K. M.; Bader, S. J.; Buchan, Z. A.; Taylor, C. E.; Montgomery, J. A Streamlined Strategy for Aglycone Assembly and Glycosylation. *Angew. Chem., Int. Ed.* **2013**, *52* (51), 13647−13650. C2' silyl linkers deliver glycosylated mono-ols via a 5-membered ring transition states, but have not been explored for diols, i.e. larger rings. See:
(34) Walk, J. T.; Buchan, Z. A.; Montgomery, J. Sugar Silanes: Versatile Reagents for Stereocontrolled Glycosylation via Intramolecular Aglycone Delivery. *Chem. Sci.* **2015**, *6* (6), 3448−3453.
(35) Ishiwata, A.; Munemura, Y.; Ito, Y. NAP Ether Mediated Intramolecular Aglycon Delivery: A Unified Strategy for 1,2-Cis-Glycosylation. *Eur. J. Org. Chem.* **2008**, *2008* (25), 4250−4263. An alternative system for C2' delivery via a mixed acetal requires acidic or hydrogenolytic deprotection, which is not well tolerated by **4**. See:
(36) Pracht, P.; Bohle, F.; Grimme, S. Automated Exploration of the Low-Energy Chemical Space with Fast Quantum Chemical Methods. *Phys. Chem. Chem. Phys.* **2020**, *22* (14), 7169−7192.
(37) Luchini, G.; Alegre-Requena, J. V.; Funes-Ardoiz, I.; Paton, R. S. GoodVibes: Automated Thermochemistry for Heterogeneous Computational Chemistry Data. *F1000Res.* **2020**, *9*, 291.
(38) Lemanski, G.; Ziegler, T. Prearranged Glycosides, Part 12, Intramolecular Mannosylations of Glucose Derivatives via Prearranged Glycosides. *Helv. Chim. Acta* **2000**, *83* (10), 2655−2675.
(39) Lemanski, G.; Ziegler, T. Synthesis of Pentasaccharide Fragments Related to the O-Specific Polysaccharide of Shigella Flexneri Serotype 1a. *Eur. J. Org. Chem.* **2006**, *2006* (11), 2618−2630.
(40) Liu, H.-J.; Yip, J.; Shia, K.-S. Reductive Cleavage of Benzyl Ethers with Lithium Naphthalenide. A Convenient Method for Debenzylation. *Tetrahedron Lett.* **1997**, *38* (13), 2253−2256.
(41) Taunton, J.; Wood, J. L.; Schreiber, S. L. Total Syntheses of Di- and Tri-O-Methyl Dynemicin A Methyl Esters. *J. Am. Chem. Soc.* **1993**, *115* (22), 10378−10379.
(42) Tamai, H.; Ando, H.; Tanaka, H.-N.; Hosoda-Yabe, R.; Yabe, T.; Ishida, H.; Kiso, M. The Total Synthesis of the Neurogenic Ganglioside LLG-3 Isolated from the Starfish Linckia Laevigata. *Angew. Chem., Int. Ed.* **2011**, *50* (10), 2330−2333.
(43) Fujitani, B.; Hanaya, K.; Higashibayashi, S.; Shoji, M.; Sugai, T. Construction of 2,6,9,11-Tetraoxatricyclo[6.2.1.$0^{3,8}$]Undecane Containing 4-Keto-D-Glucose Skeleton. *Tetrahedron* **2017**, *73* (51), 7217−7222.
(44) (a) Bottcher, T. An additive definition of molecular complexity. *J. Chem. Inf. Model.* **2016**, *56*, 462−470. (b) Demoret, R. M.; Baker, M. A.; Ohtawa, M.; Chen, S.; Lam, C. C.; Khom, S.; Roberto, M.; Forli, S.; Houk, K. N.; Shenvi, R. A. Synthetic, mechanistic, and biological interrogation of Ginkgo biloba chemical space en route to (−)-bilobalide. *J. Am. Chem. Soc.* **2020**, *142* (43), 18599−18618.
(45) Stakanovs, G.; Blazevica, A.; Belyakov, S.; Rasina, D.; Jirgensons, A. Semisynthesis of Linariophyllenes A−C and Rumphellolide H, Structure Revisions and Proposed Biosynthesis Pathways. *J. Nat. Prod.* **2023**, *86* (10), 2368−2378.
(46) Konishi, M.; Imamura, A.; Fujikawa, K.; Ando, H.; Ishida, H.; Kiso, M. Extending the Glucosyl Ceramide Cassette Approach: Application in the Total Synthesis of Ganglioside GalNAc-GM1b. *Molecules* **2013**, *18* (12), 15153−15181.
(47) https://github.com/shenvilab/autodft.
(48) Li, C.; Shenvi, R. Total Synthesis of Twenty-Five Picrotoxanes by Virtual Library Selection. *ChemRxiv* **2024**. .
(49) Anonymous Referee #5 summarized this workflow as "[a combination of] what is 'easy to calculate' with what is 'useful to calculate'," which is a good description.

https://doi.org/10.1021/jacs.4c15719
J. Am. Chem. Soc. 2025, 147, 1327−1333